Observation of pion-related effects in the photofission of preactinide nuclei

J. D. T. Arruda-Neto,* T. Saito, M. Sugawara, T. Tamae, H. Miyase, K. Abe, K. Takahisa, O. Konno, and M. Oikawa
Laboratory of Nuclear Science, Tohoku University, Sendai, Japan

S. Simionatto
Physics Institute, University of São Paulo, São Paulo, Brazil
(Received 3 August 1992)

The absolute electrofission cross sections of Au and Ta were measured in the range 25–180 MeV. The deduced photofission cross section shows, for both Au and Ta, a pronounced dip around the photopion threshold (~140 MeV). This (γ,f) dip is interpreted as a consequence of a probable photopion absorption in a "stopped pion regime."

PACS number(s): 24.75.+i, 25.85.Jg, 27.80.+w

I. INTRODUCTION

A. Pions inside the nuclear medium

The behavior of pions *inside* the nuclear medium has an ever increasing interest [1,2]. However, pions interact so strongly that whatever process they induce is likely to originate in nucleons in the low-density nuclear surface. In contrast to hadron induced interactions, on the other hand, the weakness of the electromagnetic interaction (in electroinduced and photoinduced processes) entails an illumination of the entire nuclear volume and comparatively small distortion effects. Thus, since nuclear matter is very transparent to photons, pion photoproduction would occur, in principle, with equal probability in the whole nuclear volume, with the nucleons acting as *pion radiators.* This would allow the study of the behavior of pions in the *dense portion* of the nuclear medium, too. Such a possibility is still not explored.

In the present paper this issue is addressed, by means of both (1) an original data analysis of electrofission experiments and (2) the important connection existing between the physics associated with pion absorption and photon absorption in the nucleus [2].

B. Studying pions with photofission

Above ~140 MeV (the photopion threshold) the nuclear photoabsorption takes place by means of two mechanisms: quasideuteron and pion production, where the latter dominates [3].

The decay channels characteristics of a nucleus following photoexcitation depend on the amount of *energy deposited* (nuclear excitation energy E_x) which, by its turn, is closely related to the photoexcitation mechanisms. In this regard, we note that the magnitude of E_x will depend drastically on the mean free path of the photoproduced pion (λ_π) inside the nucleus, which determines if the pion escapes or not from the nucleus—an escaping pion would carry away at least 140 MeV.

Therefore, the behavior of E_x, as a function of the incident photon energy ω, could tell us if the photopion was reabsorbed or not—in the case of reabsorption, it is possible to know if this process was followed by the emission of fast particles. In this context we observe that the fission probability of preactinide nuclei is a strong function of E_x (as discussed at length elsewhere [4–7]) and, thus, the observation of structures in the photofission cross section $\sigma_{\gamma,f}$ is directly related to corresponding structures in the function $E_x(\omega)$—this issue is retaken below.

In fact, the role played by the photopion production in the fission of ^{209}Bi and ^{208}Pb was addressed by us elsewhere [4,6]. It was observed, for these preactinide nuclei, structures in the photofission cross sections curves at $\omega \approx 200$–220 MeV, which were interpreted as signatures of the drastic fall of λ_π at $T_\pi \approx 50$–70 MeV (pion kinetic energy). Above these T_π region λ_π is smaller than the nuclear radius [8], which greatly enhances the probability of the photopion reabsorption. These findings motivated us to perform detailed electrofission cross section measurements for two other preactinides, Au and Ta, in order to delineate the systematics for this pion related structure in the photofission cross section around $\omega \approx 200$–220 MeV. The systematics was established and, in addition, the data interpretation strongly suggested the occurrence of fine thermalization effects between 200 and 220 MeV—the results will be published soon [9].

In this paper we report on the observation of *new,* and quite unexpected, (γ,f) structures near the photopion threshold (~140 MeV), which cannot be explained on the basis of known cooling-down mechanisms of the nucleus, like preequilibrium emissions and small photopion absorption probability (described by λ_π). As we show below, the only possible explanation for such (γ,f) structures is found in terms of an analogy with the known "stopped pion absorption" mechanism.

*Permanent address: Physics Institute, University of São Paulo, São Paulo, Brazil.

C. Stopped pions absorption

At photon energies $\omega > 140$ MeV, the photoproduced Δ decays back into a pion-nucleon pair ($\Delta \rightarrow N + \pi$). However, as pointed out by Bauer [2], in the presence of a second nucleon, the emitted pion has not necessarily to be on shell, but may remain virtual and be reabsorbed. If this happens, the final state contains no pion—instead, two fast nucleons will be emitted sharing the energy and momentum of the primary Δ.

Considering now pion induced reactions, we know that pion absorption on nuclei is dominated by the quasifree analog of the elementary process of pion absorption

$$\pi + d \rightarrow \Delta + N \rightarrow N + N \ ,$$

which itself is dominated by Δ production. Thus, besides scattering, the pion may also disappear within a nucleus; this process has been the subject of experimental and theoretical investigations since the 1970s and has not been well understood yet [1,2].

Another part of the pion absorption process which has received considerable attention is the absorption of stopped negative pions (details in Ref. [1]). For stopped pions, absorption is the only available channel; in this case, the delta resonance (which is dominant for fast pions) is likely to be much less important. We would like to confront this statement for *stopped pions* (absorption as the only available channel), with the peculiarities of the *photopions* produced by the absorption of photons with energies around 140–150 MeV; these pions would have kinetic energies between 0 and 10 MeV and, as a consequence, mean free paths $\lambda_\pi > 15$ fm [8]. Since the nuclear radii of preactinides are $\sim 6-8$ fm, we conclude that these photopions have a high probability of *escaping* from the nucleus. However, under such conditions (the loss of nearly all the incoming photon energy), the occurrence of fission decay (photofission) is very unlike. For nuclei with high fission barriers ($\sim 25-30$ MeV), like the preactinides, energy deposition of several tens of MeV larger than the fission barrier is required in order to give a detectable fission cross section. We evidence that the photofission cross section of preactinides like, e.g., the ^{209}Bi is ~ 1 mb at $\omega \approx 140$ MeV, and that in the energy interval 100–160 MeV the cross section increases by one order of magnitude [4,5].

Therefore, we are led to conclude that the photopions produced near the threshold (~ 140 MeV) are predominantly absorbed; in other words, these photopions remain off shell and are reabsorbed. Based on all these experimental evidences and reasonings, we propose a very simple explanation for the photopion reabsorption mechanism near the threshold. In fact, at $\omega \approx 140$ MeV the photoproduced pion has $T_\pi \approx 0$, which is kinematically similar to a *stopped pion;* so, since *absorption* is the only available channel for stopped pion, it may well be possible that near-threshold photopions are absorbed in some sort of "stopped pion regime"—experimental evidences are presented below.

II. THEORETICAL ASPECTS

In the intermediate energy region ($\omega \gtrsim 100$ MeV), the absorption of a photon initiates an intranuclear cascade in which particles of the continuum leave the nucleus (preequilibrium emission) all along until equilibration [7,10] (compound nucleus formation with excitation energy $E_x < \omega$). Thus, we propose to write the photofission cross section as

$$\sigma_{\gamma,f}(\omega) = \sum_{A_c,Z_c} \sum_i N(E_{xi},\omega)\sigma_{\rm CN}(A_c,Z_c;E_{xi}) \times P_f(A_c,Z_c;E_{xi}) \ , \quad (1)$$

where A_c and Z_c are the atomic masses and atomic numbers of the compound nuclei, respectively, $\sigma_{\rm CN}$ is the cross section for compound nucleus formation, P_f is the fission probability of the compound nucleus (A_c,Z_c), and $N(E_{xi},\omega)$ is the probability of finding a compound nucleus with excitation energy equal to E_{xi}; also, it represents the E_x distribution in the energy interval $0-\omega$. Recently, Guaraldo and co-workers [7,10,11] performed detailed calculations to obtain $N(E_x,\omega)$ for several nuclei in the range of $\omega = 100-300$ MeV. It was used the intranuclear cascade model with the inclusion of the two leading photoexcitation mechanisms: quasideuteron photoabsorption and single nucleon photoabsorption via pion production on intranuclear nucleons. The results for $N(E_{xi},\omega)$ were presented as histograms centered at E_{xi}.

In the ω energy range pertinent to this paper (around the photopion threshold), the A_c and Z_c distributions are very sharp. In fact, at $\omega \approx 150$ MeV for ^{197}Au we have [7]

$$\Delta A_c = A_t - \overline{A}_c \simeq 1.4 \ , \quad (2)$$

$$\Delta Z_c = Z_t - \overline{Z}_c \simeq 0.5 \ , \quad (3)$$

where A_t and Z_t refer to the target nucleus. Thus, we can simplify our theoretical approach by assuming that *only one* compound nucleus $(\overline{A}_c,\overline{Z}_c)$, a "mean compound nucleus," was formed. Next, following a formalism developed by Kikuchi and Kawai [12], plus our "mean compound nucleus" assumption, we get

$$\frac{\sigma_{\rm CN}(E_x)}{E_x} = \frac{\sigma_{\gamma,a}(\omega)}{\omega} \ , \quad (4)$$

where $\sigma_{\gamma,a}$ is the photoabsorption cross section.

Substituting $\sigma_{\rm CN}$, from Eq. (4), in Eq. (1) we obtain

$$\sigma_{\gamma,f}(\omega) = \frac{\sigma_{\gamma,a}(\omega)}{\omega} \sum_i N(E_{xi},\omega)E_{xi}P_f(\overline{A}_c,\overline{Z}_c;E_{xi}) \ . \quad (5)$$

Furthermore, we know from Refs. [7,10] that the E_x distributions $N(E_x,\omega)$ for $\omega \gtrsim 180$ MeV are broad, while for $\omega < 180$ MeV they are relatively sharper. Thus, our next and last approximation is to replace the distributions of E_x by its average value $\overline{E}_x$, where

$$\overline{E}_x(\omega) = \sum_i N(E_{xi},\omega)E_{xi} \ . \quad (6)$$

Finally, for $\omega < 180$ MeV, Eq. (5) takes the following simple form,

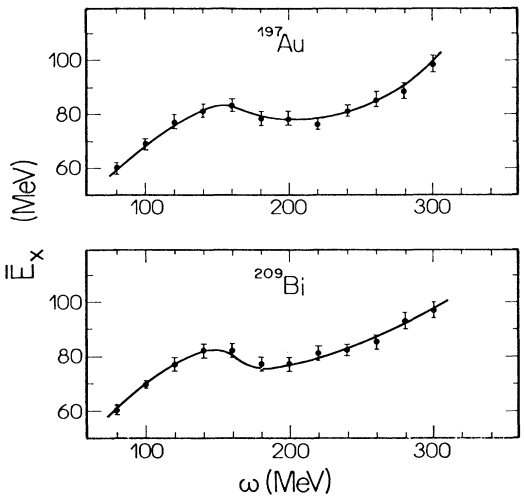

FIG. 1. Average excitation energy $\bar{E}_x$ as a function of the incident photon energy ω, for ^{197}Au and ^{209}Bi target nuclei (from Refs. [7,11]).

$$\sigma_{\gamma,f}(\omega)\cong\sigma_{\gamma,a}(\omega)\left[\frac{\bar{E}_x(\omega)}{\omega}\right]P_f(\bar{A}_c,\bar{Z}_c;\bar{E}_x)\ . \tag{7}$$

It is important to point out that (a) $\sigma_{\gamma,a}(\omega)$ exhibits no structure for $\omega\cong 100-300$ MeV [3,13], (b) $\bar{E}_x$ as a function of ω is structureless too, up to $\omega\cong 160$ MeV, as shown in Fig. 1 (quoted from Ref. [7]), and (c) it is a well-known fact that P_f, for a preactinide nucleus, is a smooth and steep rising function (nearly exponential) of E_x [14]. Therefore, from both experimental and theoretical points of view, known to date, the photofission cross section is a smooth function of ω in the 100–160 MeV range. This conclusion is of paramount importance when confronted with the experimental findings of the present work; this will be discussed in the subsequent sections.

III. EXPERIMENT AND RESULTS

Targets of Au and Ta with high purity, ~ 2.5 mg/cm^2 thick each, were irradiated with the electron beam of the Tohoku University Linac (Sendai) with energies from 40 to 250 MeV in steps of 5 and 10 MeV, using mica foils as fission detectors. The electron beam was monitored by means of a ferrite core monitor absolutely calibrated to $\pm 1\%$. The target thicknesses were determined by the well-known x-ray attenuation method, using ^{57}Co as the x-ray source and a hyperpure germanium detector; accuracies around 3% were achieved. We refer the reader to Ref. [4] for more experimental details.

This paper deals with a peculiar behavior of photopions near the threshold (~ 140 MeV). Above 170 MeV the electrofission process is dominated by fine characteristics of the nuclear thermalization process; this subject lies beyond the scope of the present work. In fact, a comprehensive approach on "thermalization related effects" is in the process of publication elsewhere [9]. Therefore, we will restrict our data analysis and interpretation for electron energies E_e up to 170 MeV.

Since a reliable unfolding of the (γ,f) cross section requires (e,f) data down to the fission barrier (~ 25 MeV), we performed electrofission cross section measurements of Au and Ta, in the interval 25–40 MeV, with the electron beam of the University of São Paulo Linac and with the same targets used in Sendai. We note in passing that the difficulties associated with possible $(e,e'f)$ exclusive measurements of preactinide nuclei have been pointed out elsewhere [15]. Typical single-armed fission cross sections range from 10^{-3} to 1 μb; if coincidence is imposed, the $(e,e'f)$ cross sections become several orders of magnitude lower than those for (e,f), which makes these experiments very time consuming.

Our results for the (e,f) cross sections $\sigma_{e,f}$ of Au and Ta are shown in Fig. 2. Also shown in Fig. 2 are the preliminary results for the electrofission of ^{232}Th [16], obtained in Sendai with the same experimental setup used for Au and Ta—the reason for these data to be shown will be explained below.

The most striking feature of our (e,f) data are the somewhat unexpected inflexions around m_π, which correspond to structures in the photofission cross sections $\sigma_{\gamma,f}$, because

$$\sigma_{e,f}(E_e)=\int_0^{E_e}\sigma_{\gamma,f}(\omega)N^{E1}(E_e,\omega)\frac{d\omega}{\omega}\ , \tag{8}$$

where $N^{E1}(E_e,\omega)$ is the $E1$ virtual photon spectrum. These (γ,f) structures are, in fact, present in the data from Frascati [5] and Kharkov [17] but they were not recognized (see Fig. 3). Keeping in mind, for the moment, only our (e,f) results for Au and Ta, we would like to discuss next the "statistical significance" of the observed inflexions and, at the same time, to what extent it is possible to discard the so-called "fluctuation artifacts." In this regard we stress the following points.

(1) The reproducibility of the (e,f) experimental points is better than 5%.

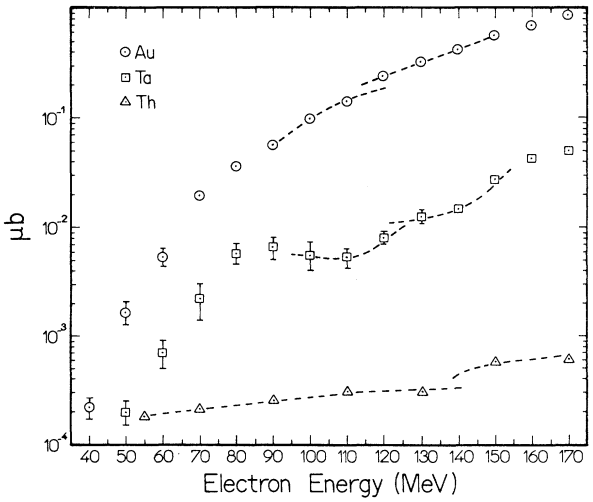

FIG. 2. Electrofission cross sections of Au and Ta (this work), and preliminary (e,f) data of Th [16] (arbitrary units), for comparison purposes (see text). The dashed lines are to guide the eye.

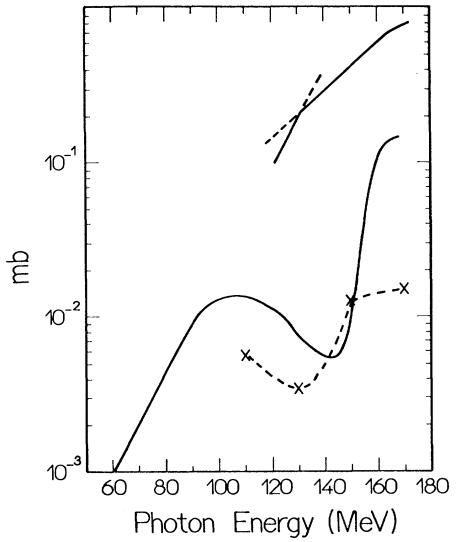

FIG. 3. Photofission cross section of Au deduced in this work (solid curve; average uncertainties are ~15%) and from Ref. [17] (×---×). Also shown the Au photofission yield per equivalent quantum versus the maximum photon energy, measured at Frascati (right top corner; adapted from Ref. [5]; arbitrary units).

(2) The (e,f) curves of preactinides are steep functions of the energy, which makes the presence of inflexions much more evident.

(3) This experiment was planned in such a way that, by measuring two preactinides in *two independent experiments,* each one of the nuclei works as a *veto* to the other. In this sense, an observed inflexion is accepted as a "physical fact" (and not a possible fluctuation) only if is observed in *both nuclei* and at the *same energy position.* Instrumental fluctuations in the yield curves could be attributed only to possible problems in the beam monitor and/or energy control devices. However, these equipment pieces were routinely checked before and after each run.

(4) The inclusion in Fig. 2 of the preliminary ^{232}Th(e,f) data [16] has the intention of reinforcing the conviction that near-photopion threshold (e,f) inflexions are general characteristics of heavy nuclei (both preactinides and actinides).

(5) A simulation (described in Sec. IV A) for the (e,f) curves points to the statistical significance of the observed inflexions, too.

IV. DATA ANALYSIS AND INTERPRETATION

A. Simulation of an inflexionless (e,f) curve

A linear plot of (e,f) data around the inflexions is shown in Fig. 4. A mere visual inspection shows that the existence of a Ta(e,f) inflexions is out of question. In the case of the Au(e,f) data, we demonstrate below that the inflexion is delineated by the near totality of the experimental points between 90 and 140 MeV.

In fact, we note that the Au(e,f) points could be assembled into two groups, where each group of points

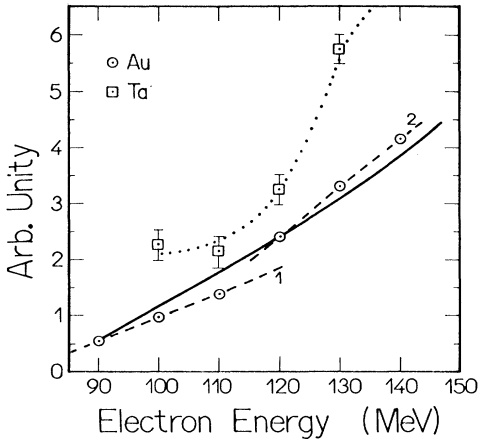

FIG. 4. Linear plot of the (e,f) data shown in Fig. 2 for Au and Ta. The dashed and dotted lines are to guide the eye. The solid curve is the result of a calculation which simulates an inflexionless (e,f) curve (details in the text).

defines a straight line (dashed lines 1 and 2 in Fig. 4). The slopes of these straight lines are very different: they are equal to 22° and 41° for lines 1 and 2, respectively.

Another statistical analysis of the inflexions is provided by the comparison between the experimental curve and an inflexionless calculated curve. This curve is obtained by integration of a semitheoretical $\sigma^*_{\gamma,f}$ cross section with the virtual photon spectrum [Eq. (8)], where $\sigma^*_{\gamma,f}$ is calculated from the expression [Eq. (7)]

$$\sigma^*_{\gamma,f}(\omega)=\sigma_{\gamma,a}(\omega)\left[\frac{\bar{E}_x(\omega)}{\omega}\right]P_f \ . \tag{9}$$

We took $\sigma_{\gamma,a}$ from experimental results [13,18] and we know from calculations that $\bar{E}_x/\omega$ is nearly constant [7,10]. The fission probability energy dependence is nearly proportional to $\exp(a\sqrt{\bar{E}_x})$ [14]; thus, we can write

$$\sigma^*_{\gamma,f}(\omega)=b\sigma_{\gamma,a}(\omega)\{\exp[a\sqrt{\bar{E}_x(\omega)}]\} \ , \tag{10}$$

where a and b are constants.

After integration of this structureless photofission cross section with $N^{E1}(\omega,E_e)$, as in Eq. (8), we obtain an inflexionless (e,f) curve $\sigma^*_{e,f}$. The full curve shown in Fig. 4 is the best fit of $\sigma^*_{e,f}$ to the data points, using a and b as fitting parameters; the corresponding reduced χ^2 is ~10 demonstrating, therefore, that the experimentally observed inflexion is statistically significant.

B. Restoration of (γ,f) from (e,f): unfolding

First of all, we would like to emphasize that the unfolding of $\sigma_{\gamma,f}$ from $\sigma_{e,f}$ [Eq. (8)], is necessary only for quantitative analysis purposes, since the visual inspection of the (e,f) curve (Figs. 2 and 4) has already revealed the existence and location of the (e,f) structure. In Fig. 3 is shown the unfolded (γ,f) cross section of Au, obtained by means of a least-structure unfolding technique developed at this laboratory; we used virtual-

photon spectra calculated in the distorted-wave Born approximation with the inclusion of nuclear size effects [19]. A prominent dip is observed for Au around 140–145 MeV, and for Ta around 150 MeV (not shown in Fig. 3).

Also, in Fig. 3 are shown (γ,f) curves derived from three different set of data: electrofission (this work), bremsstrahlung induced fission (Kharkov), and photofission with quasimonochromatic photons (Frascati). The data points from Frascati correspond to the yield curve (integral of $\sigma_{\gamma,f}$ over the photon spectrum), which needs to be deconvoluted—however, the occurrence of an inflexion is pointing to a (γ,f) structure dip around 130–140 MeV, which compares well with our reported finding at 140–145 MeV.

Examining again Eq. (7) (plus the discussion in Sec. IV A), we come to the conclusion that structures in the photofission curve are certainly due to corresponding structures of $\bar{E}_x$ as a function of $\omega(\bar{E}_x X\omega)$. However, the calculated $\bar{E}_x X\omega$ curves shown in Fig. 1 are structureless around 140 MeV indicating, thus, that the intranuclear cascade (INC) calculations of Guaraldo *et al.* [7] did not take into account *all* possible photoexcitation mechanisms. As discussed below, there must be a *new effect* responsible for a drastic reduction of the excitation energy at $\omega\approx 140$ MeV.

C. Photofissility

The photofissility W_f is defined as

$$W_f(\omega)=\frac{\sigma_{\gamma,f}(\omega)}{\sigma_{\gamma,a}(\omega)} . \tag{11}$$

We calculated W_f for Au and Ta from the unfolded $\sigma_{\gamma,f}$, and $\sigma_{\gamma,a}$ from the literature—results are in Fig. 5. The analysis of the photofissility is very interesting because of its simple form, as derived from Eq. (7):

$$W_f(\omega)=\left[\frac{\bar{E}_x(\omega)}{\omega}\right]P_f(\bar{A}_c,\bar{Z}_c;\bar{E}_x) . \tag{12}$$

Thus, the fine characteristics (e.g., structures) of W_f are dictated by the interplay between the *energy absorbed* by the target nucleus (ω), and the *energy deposited* (E_x) in the thermalized systems (the compound nucleus). Therefore, the dip around $\omega=140$ MeV (see Fig. 5) indicates that the nucleus looses an "extra" amount of excitation energy, not predicted by the INC calculations shown in Fig. 1.

The "extra amount" of excitation energy lost around $\omega=140$ MeV is estimated to be ~ 55 MeV because (see Fig. 5)

$$W_f(\omega\cong 140\text{ MeV})=W_f(\omega\cong 85\text{ MeV}) .$$

D. Stopped pion absorption regime

We propose an explanation for the dip in the photofissilities of Au and Ta, around 140 MeV, in terms of an analogy with the well-known stopped pion absorption regime in the nucleus. In support to this idea we

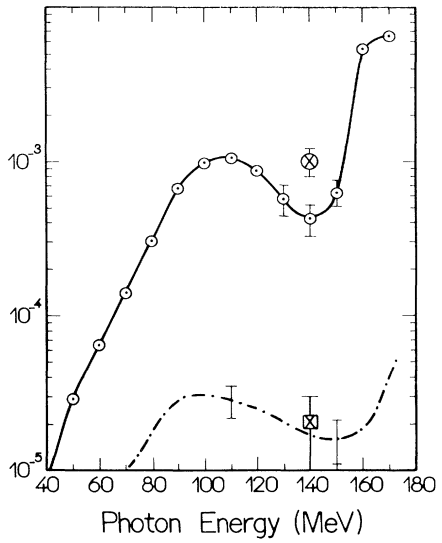

FIG. 5. Photofissilities W_f of Au (⊙–⊙) and Ta (–·–) as a function of the incident photon energy (deduced in this work); typical uncertainties are shown only for the dip region. Probabilities of fission induced by stopped negative pion absorption in Au (⊗) and Ta (⊠), quoted from Ref. [20].

mention the following experimental evidences.

(a) The kinematics of the photoproduced pions around the threshold (where the dip is located) is similar to stopped pions (details in Sec. I C).

(b) According to the quasideuteron model for pion absorption, a pion is absorbed by a pair of nucleons in the nucleus while the remaining nucleons act as spectators. This process is accompanied by the formation of several particles which can be emitted, rescattered or absorbed by the nucleus. In fact, the experimentally obtained spectrum of neutrons formed as a result of the absorption of stopped negative pions by the preactinide nucleus ^{208}Pb (see Fig. 2 of Ref. [20]) exhibits three groups of neutrons: evaporation stage nucleons, preequilibrium emission neutrons ($T_n\approx 20$–40 MeV) and cascade stage neutrons (fast neutrons with $T_n\gtrsim 50$ MeV). This last group of fast neutrons shows a distinct peak at $T_n\cong 55$ MeV, which compares well with the amount of "extra" loss of energy (as estimated above).

(c) The experimentally obtained fission probability of Au and Ta by stopped negative pions, $P_f(\pi^-)$, is shown in Fig. 5 (quoted from Fig. 10 of Ref. [20]). Taking an average of W_f around the dip region, an excellent agreement between $P_f(\pi^-)$ and $\langle W_f\rangle$ is achieved.

It is worth mentioning that there is to date no alternative photoabsorption mechanism to explain our experimental findings. Therefore, the compelling evidences discussed above suggest that we have detected a *stopped pion absorption regime* in the photofission of Au and Ta near the photopion threshold.

From the arguments presented in Sec. I C, it is quite evident that the photopions produced near the threshold are predominantly absorbed. Now, we are showing that these pions are absorbed in a stopped pion regime. Since photopions are produced in the whole nuclear volume,

we are led to conclude that the absorption characteristics of stopped pions at the less dense nuclear surface, are *similar* to those at the dense portion of the nuclear matter. This is particularly true if we note that $P_f(\pi^-) \cong \langle W_f \rangle$, as discussed above (see also Fig. 5). In fact, the incoming energy is the same in both situations (140 MeV) and, since the available energy to fission is also the same [because $P_f(\pi^-) \cong \langle W_f \rangle$], it becomes obvious that the energies of the emitted particles (e.g., protons and neutrons from the splitted quasideuteron) are comparable for both processes: stopped pions absorption at the nuclear surface, and "stopped photopions" in the nuclear interior.

E. Possibilities for the existence of a fission related structure around $\omega = 140$ MeV

Since our interpretation for the observed (γ,f) dip around 140 MeV, in terms of a stopped pion regime, rely on the assumption that the fission probability is a strongly rising function of the excitation energy (E_x) for preactinide nuclei, we would like to discuss with more details the correctness of this assumption.

The fission probability would decrease for an increasing E_x if substantially less fissionable residual systems are formed, which is not the case in the energy region around the (γ,f) dip, where $E_x < 85$ MeV (see Fig. 1) and the momenta transferred to the nucleus are $\lesssim 160$ MeV/c. In fact, for, e.g., ^{197}Au(γ,f) the most probable residual nuclei (compound nuclei, in this case) formed for $E_x < 85$ MeV are ^{197}Au, ^{196}Au, and, to a less extent, ^{195}Pt, since $\Delta A_c \simeq 1.4$ and $\Delta Z_c \simeq 0.5$, as discussed in Sec. II. All these nuclei have comparable fissilities; the fission rate is simply determined by the level densities and the available energy (E_x less the fission barrier height). For low and "moderately" low excitation energies ($E_x \lesssim 50$–80 MeV), the relative probability for fission compared to neutron emission is a strongly increasing function of E_x (see Table VII-1 of Ref. [22] and, in particular, the compound nucleus ^{179}Ta).

Also, fission events following photopion emission, at $\omega \simeq 140$–160 MeV, are nearly nondetectable (see discussion in Sec. I C), because the excitation energies would be $\lesssim \omega - m_\pi$, while the fission barrier heights for Au and Ta are ~ 30 MeV—therefore, only sub-barrier fission is expected to occur, which lies below the lower limit of our detection sensitivity.

Finally, the so-called "saturation effects" in the fission probability are likely to manifest above $E_x = 100$–200 MeV, where pre-equilibrium emission of heavy fragments (the nuclear fragmentation), and/or the fast nucleon cascade, leads to residual systems that are too light, and/or too cold, to fission. In this regard, we refer the reader to the recent fission decay calculations performed by Blaich *et al.* [21] for heavy-ion reactions at intermediate energies. These calculations involve an intranuclear cascade, subsequent fast nucleon emission, and final decay by statistical evaporation including fission (using the PACE statistical model code). From 300 to 150 MeV of excitation energy fission is not allowed to compete as a decay channel. This choice is made as a simple approximation for the dissipative and flow dynamic effects that impose minimum times for fission to become a viable decay channel (Ref. [21] and references therein). On the other hand, for $E_x < 150$ MeV, fission is allowed as a decay channel in PACE. These calculations were able in reproducing important characteristics of fission data from 100 MeV/nucleon reactions, with Fe and Nb projectiles, on targets of Ta, Au, and Th (the same three targets investigated with photofission—see Fig. 2).

Therefore, from the above-mentioned facts, we can conclude that our assumption for P_f (a strongly rising function of E_x) is valid for $E_x < 85$ MeV, at least, since significant slowing down of the fission process (as compared to expectations based on the statistical model) in this excitation energy region is unlikely.

V. FINAL REMARKS

As final remarks, we would like to recall that this paper deals with three distinct issues.

(1) Experimental results. The (γ,f) cross sections of Au and Ta were obtained from their corresponding (e,f) cross sections, revealing the existence of dips around the photopion threshold.

(2) Theoretical approach. It was developed an expression for the photofission cross section [Eq. (7)], where the quantities describing the photoexcitation process ($\sigma_{\gamma,a}$) the thermalization stage (E_x), and the fission decay of the thermalized system (P_f), were factorized allowing, therefore, a better understanding of the importance of each stage in the whole (γ,f) process.

(3) Suggestion for a new effect. We suggested an explanation for the existence of (γ,f) dips around the photopion threshold, by means of a simple analogy with the stopped pion absorption process—several evidences for this new effect were presented.

Given the subtle nature of the reported inflexions, and the uncertainties associated to the experiment itself (particularly for Ta), it is our hope that further (e,f) and (γ,f) experiments could be pursued by other groups allowing, thus, the confirmation or not of our findings.

ACKNOWLEDGMENTS

We would like to thank the Linac crew for providing the specified electron beam. This work was partially supported by the Conselho Nacional de Desenvolvimento Científico e Tecnológico (Brazil) and the Japan Society for the Promotion of Science.

[1] D. Ashery and J. P. Schiffer, Ann. Rev. Nucl. Part. Sci. **36**, 207 (1986).

[2] T. S. Bauer, Nucl. Phys. **A546**, 181c (1992).

[3] J. Ahrens, H. Gimm, R. H. Hughes, R. Leicht, P. Minn, A. Zieger, and B. Ziegler, in *Photopion Nuclear Physics,* edited by P. Stoler (Plenum, New York, 1979), p. 385.

[4] J. D. T. Arruda-Neto, M. Sugawara,, T. Tamae, O. Sasaki, H. Ogino, H. Miyase, and K. Abe, Phys. Rev. C **34**, 935

(1986).
[5] V. Lucherini, C. Guaraldo, E. De Sanctis, P. Levi Sandri, E. Polli, A. R. Reolon, A. S. Iljinov, S. Lo Nigro, S. Aiello, V. Bellini, V. Emma, C. Milone, G. S. Pappalardo, and M. V. Mebel, Phys. Rev. C **39**, 911 (1989).
[6] J. D. T. Arruda-Neto, M. Sugawara, H. Miyase, T. Kobayashi, T. Tamae, K. Abe, M. Nomura, H. Matsuyama, H. Kawahara, K. Namai, M. L. Yoneama, and S. Simionatto, Phys. Rev. C **41**, 354 (1990).
[7] C. Guaraldo, V. Lucherini, E. De Sanctis, A. S. Iljinov, M. V. Mebel, and S. Lo Nigro, Nuovo Cimento **103A**, 607 (1990).
[8] A. M. Bernstein, in *Photopion Nuclear Physics,* edited by P. Stoler (Plenum, New York, 1979), p. 406.
[9] J. D. T. Arruda-Neto, T. Saito, M. Sugawara, T. Tamae, H. Miyase, K. Abe, K. Takahisa, O. Konno, M. Oikawa, and S. Simionatto (unpublished).
[10] A. S. Iljinov, M. V. Mebel, C. Guaraldo, V. Lucherini, E. De Sanctis, N. Bianchi, P. Levi Sandri, V. Muccifora, E. Polli, A. R. Reolon. P. Rossi, and S. Lo Nigro Phys. Rev. C **39**, 1420 (1989).
[11] V. Lucherini, private communication.
[12] K. Kikuchi and M. Kawai, *Nuclear Matter and Nuclear Reactions* (North-Holland, Amsterdam, 1968), p. 244.
[13] C. Chollet, J. Arends, H. Beil, R. Bergère, P. Bourgeois, P. Carlos, J. L. Fallou, J. Fagot, P. Garganne, A. Leprête, and A. Veyssière, Phys. Lett. **127B**, 331 (1983).
[14] S. Bjornholm and J. E. Lynn, Rev. Mod. Phys. **52**, 725 (1980).
[15] J. D. T. Arruda-Neto, M. Sugawara, H. Miyase, T. Kobayashi, T. Tamae, K. Abe, M. Nomura, H. Matsuyama, H. Kawahara, K. Namai, M. L. Yoneama, and S. Simionatto, J. Phys. G **15**, L215 (1989).
[16] J. D. T. Arruda-Neto, T. Saito, M. Sugawara, T. Tamae, H. Miyase, K. Abe, K. Takahisa, O. Konno, M. Oikawa, and S. Simionatto (unpublished).
[17] Yu. N. Ranyuk and V. Soronkin, Yad. Fiz. **5**, 37 (1966) [Sov. J. Nucl. Phys. **5**, 26 (1966)].
[18] A. Leprêtre, H. Beil, R. Bergère, P. Carlos, J. Fagot, and A. Veyssière, Nucl. Phys. **A390**, 240 (1982).
[19] F. Zamani-Noor and D. S. Onley, Phys. Rev. C **33**, 1354 (1986).
[20] A. S. Iljinov, V. I. Nazaruk, and S. E. Chigrinov, Nucl. Phys. **A268**, 513 (1976).
[21] Th. Blaich, M. Begemann-Blaich, M. M. Fowler, J. B. Wilhelmy, H. C. Britt, D. J. Fields, L. F. Hansen, M. N. Namboodiri, T. C. Sangster, and Z. Fraenkel, Phys. Rev. C **45**, 689 (1992), and references therein.
[22] R. Vandenbosch and J. R. Huizenga, *Nuclear Fission* (Academic, New York, 1973), pp. 254 and 255.